HHS Public Access

Author manuscript

Nat Immunol. Author manuscript; available in PMC 2014 September 01.

Published in final edited form as:

Nat Immunol. 2014 March ; 15(3): 266–274. doi:10.1038/ni.2822.

Intrinsic CD4+ T cell sensitivity and response to pathogen are set and sustained by avidity for thymic and peripheral self-pMHC

Stephen P. Persaud[1], **Chelsea R. Parker**[1], **Wan-Lin Lo**[1], **K. Scott Weber**[2], and **Paul M. Allen**[1]

[1]Department of Pathology and Immunology, Washington University School of Medicine, St. Louis, MO 63108

[2]Department of Microbiology and Molecular Biology, Brigham Young University, Provo, UT 84602

Abstract

T cell receptor (TCR) interactions with self-peptide-major histocompatibility complex (pMHC) are crucial to T cell development, but their role in peripheral T cell responses remains unclear. Specific and nonspecific stimulation of *Listeria*-specific LLO56 and LLO118 TCR transgenic T cells elicited distinct interleukin 2 (IL-2) and phospho-ERK responses, the strength of which was set in the thymus and maintained in the periphery in proportion to TCR-self-pMHC avidity. Withdrawal of self-pMHC markedly compromised LLO56 expansion to *Listeria in vivo*. Despite their markedly different self-reactivities, LLO56 and LLO118 bound cognate-pMHC with identical affinities, challenging associations made between these parameters. Our findings highlight a crucial role for selecting ligands encountered during thymic education in determining the intrinsic functionality of $CD4^+$ T cells.

Initiation of $CD4^+$ T cell responses requires productive interaction between the T cell receptor (TCR) and peptide-major histocompatibility complex class II (pMHC)[1,2]. These interactions are highly sensitive and specific despite their micromolar-range binding affinities[3]. Even weaker interactions between the TCR and self-pMHC ligands serve critical roles in T cell development, survival and peripheral function[4-8]. It is evident that the TCR can discriminate between pMHC ligands, even subtly different ones[9], to signal distinct functional outcomes. It remains an important pursuit to understand the molecular features of TCR-pMHC interactions that promote effective $CD4^+$ T cell responses to pathogens.

TCR affinity for cognate pMHC and clonal frequency in the preimmune repertoire are important factors governing the magnitude of *in vivo* $CD4^+$ and $CD8^+$ T cell responses to pathogen[10-14]. Higher-affinity $CD4^+$ and $CD8^+$ T cells, with greater functional avidity for antigen, are more prevalent after infection than before, demonstrating clear evolution of the anti-pathogen repertoire. Low-affinity interactions can also lead to generation of effector

Address correspondence to Paul M. Allen: pallen @wustl.edu.

Author Contributions S.P.P., K.S.W., and P.M.A. designed the study. S.P.P., K.S.W., W-L. L, and C.R.P. performed all experiments. S.P.P. and P.M.A. wrote the manuscript. K.S.W. performed the initial studies with the LLO TCR transgenic mice. All authors read, commented on, and approved the manuscript prior to submission.

and memory $CD8^+$ populations, albeit more slowly and to a lesser extent than their higher affinity counterparts[15].

How TCR recognition of self-pMHC affects $CD4^+$ T cell responses has received less attention, due to the weak nature of these interactions, the paucity of known endogenous selecting ligands, and the difficulty of specifically perturbing self-pMHC without also affecting presentation of cognate antigen. Functionally, the degree of TCR self-reactivity has been correlated with cell surface expression of the negative regulator CD5[16]. The expression of CD5 is set during positive selection in proportion to the strength of signal from self-pMHC perceived by the TCR, often referred to as TCR-self-pMHC "avidity." Recently, it was reported that T cells having greater avidity for self-pMHC were more readily positively selected, and that this enriched the mature repertoire with clones that bound more strongly to foreign pMHC and responded better to pathogen *in vivo*[17].

To investigate at a clonal level how TCR-pMHC interactions impact $CD4^+$ T cell responses, we used two TCR transgenic mouse lines called LLO56 and LLO118. Both lines have $CD4^+$ T cells that recognize residues 190-205 of the *Listeria monocytogenes* virulence factor Listeriolysin O bound to $I\text{-}A^b$. The TCRs were cloned from T cell hybrids generated using *Listeria*-infected B6 mice, and so represent two solutions to recognizing the same pathogen-derived cognate pMHC. These cells have a highly similar cell surface phenotype, but one notable exception is LLO56's markedly higher expression of CD5 compared to LLO118.

During primary *in vivo* responses to *Listeria*, LLO118 T cells expanded more than LLO56, which was associated with a greater propensity of LLO56 T cells to undergo cell death[18].Since strong TCR signals can induce cell death during immune responses[19], we set out in the current study to test if LLO56 T cells perceive such strong TCR signals on activation as to induce the significant cell death we previously observed. We show that in addition to specific stimuli eliciting stronger IL-2 responses from LLO56 than LLO118 T cells, nonspecific stimuli bypassing the TCR could do the same, suggesting that there were intrinsic differences in the responsiveness of the two T cells to stimulation. The stronger IL-2 responses were associated with higher phosphorylation of TCRζ at baseline and ERK upon activation. We also demonstrate that the basal signaling and responsiveness of LLO56 and LLO118 T cells were not hardwired features of these cells; rather, they were acquired during positive selection in proportion to TCR avidity for selecting self-pMHC, and required active maintenance by self-pMHC in the periphery. Together, these data suggest a crucial role for thymic education and TCR self-reactivity in determining the intrinsic functional attributes of $CD4^+$ T cells. Based upon these observations we propose a TCR-instructive model whereby selecting TCR-self-pMHC interactions establish $CD4^+$ T cell function and basal signaling centrally and maintain this functionality in the periphery, ultimately shaping how a given T cell will perform during pathogen challenge.

Results

Distinct LLO56 and LLO118 T cell IL-2 responses to TCR-bypassing stimuli

LLO56 and LLO118 T cells showed similar upregulation of the activation markers CD69 and CD25 in response to LLO peptide and αCD3+αCD28 stimulation (Fig. 1a). This is in

accord with our previous observations that LLO56 and LLO118 T cells proliferated similarly well to antigen *in vitro* and *in vivo* (Table 1 and Supplementary Fig. 1a). However, over the same peptide dose range, LLO56 T cells produced much more IL-2 than LLO118 (Fig. 1b). This could not be explained by differences in expression of the TCR, CD3, CD4 or the costimulatory molecules CD28, CTLA-4, PD-1 or PD-L1 (Supplementary Fig. 1b). One possible explanation for this was a difference in affinity of the TCR for the LLO(190-205)/I-A^b ligand. We generated soluble LLO56 and LLO118 TCRs and performed surface plasmon resonance (SPR) to determine the affinities. The affinities of the LLO56 and LLO118 TCRs for LLO(190-205)/I-A^b were identical, suggesting that the distinct IL-2 responses were not related to differences in binding to LLO/I-A^b (Fig. 1c). Thus, despite binding cognate antigen with similar affinity and receiving a similarly activating stimulus, LLO56 showed a greater ability than LLO118 to produce IL-2.

A stronger IL-2 response could also be elicited from LLO56 T cells by stimulation with αCD3+αCD28 (Fig. 1b, d). This was also true when cells were stimulated with PMA and ionomycin (P+I), which act intracellularly downstream of the TCR (Fig. 1e). LLO56 and LLO118 T cells did not differ markedly in their ability to produce interferon γ IFN-γ or TNF in response to P+I, indicating that LLO56's stronger IL-2 response could not be generalized to all cytokine responses (Fig. 1e). These findings opposed the presumption that two T cells with different TCRs would respond equally to stimuli bypassing the TCR and suggested that LLO56 and LLO118 bore intrinsic differences governing the strength of their IL-2 responses, a finding we pursued further given its potential relevance to the *in vivo* biology of these cells.

Higher Erk and basal TCRζ phosphorylation in LLO56 T cells

To mechanistically understand how nonspecific stimuli could elicit distinct IL-2 responses from LLO56 and LLO118 T cells, we investigated the signaling pathways activated by P+I expression, including the Ca^{2+}-NFAT, NF-κB, and Ras-Erk pathways. Using phosphoflow cytometry, we found that nonspecific stimulation induced higher expression of phospho-ERK from LLO56 than LLO118, with similar results obtained by immunoblot (Fig. 2a and Supplementary Fig. 2a). PMA-induced IκBα degradation (Fig. 2b) and ionomycin-induced calcium flux (Fig. 2c) were similar between LLO56 and LLO118, with LLO118 showing somewhat stronger responses in both assays. Thus, greater activation of ERK most clearly tracked with the stronger IL-2 response to P+I stimulation in LLO56 T cells.

As peptide and antibody stimulation also elicited stronger IL-2 responses from LLO56 than LLO118, we considered that there might also be differences in proximal signaling. Several studies have linked TCR self-reactivity to the extent of basal TCRζ phosphorylation[17,20,21]. Indeed, upon examination, LLO56 had higher basal levels of p21 phospho-TCRζ than LLO118 (Fig. 2d). The identity of p21 phospho-TCRζ in these experiments was confirmed using a rabbit anti-ζ serum, which recognizes both phosphorylated and unphosphorylated TCRζ species (Supplementary Fig. 2b). Taken together, these studies demonstrate both basal and inducible differences in cell signaling that are associated with LLO56's greater intrinsic IL-2 response.

Polyclonal T cell IL-2 response strength correlates with CD5 expression

Based on their respective expression of CD5 and basal TCRζ phosphorylation, we predicted that the LLO56 T cell perceives a stronger TCR signal from self-pMHC than LLO118. We hypothesized that such a signal might underlie the stronger LLO56 response to P+I stimulation. However, to test that our observations were not limited to TCR transgenic cells only, we asked whether TCR self-reactivity, as gauged by CD5 expression, correlated with the strength of the response to nonspecific stimulation in polyclonal B6 $CD4^+$ and $CD8^+$ T cells, with the prediction that $CD5^{hi}$ T cells (like LLO56) should be more responsive to P+I stimulation than $CD5^{lo}$ cells (like LLO118). We observed that $CD5^{hi}$ $CD4^+$ and $CD8^+$ T cells more readily produced IL-2 in response to P+I (Fig. 3a) or αCD3+αCD28 (Supplementary Fig. 3a) than $CD5^{lo}$ T cells. Stimulation did not markedly alter the distribution of CD5 expression on T cells (Supplementary Fig. 3b), which we confirmed using cells sorted according to their CD5 expression prior to stimulation (Supplementary Fig. 3c). Furthermore, $CD5^{hi}$ $CD4^+$ and $CD8^+$ T cells had higher expression of pERK on activation and higher basal expression of p21 phospho-TCRζ than $CD5^{lo}$ T cells (Fig. 3b,c). Because these experiments were done with bulk $CD4^+$ and $CD8^+$ T cells, which would include memory phenotype and nonconventional αβ T cells (i.e., regulatory T cells (T_{reg} cells), NKT cells), we repeated these analyses using magnetically- or flow cytometry-sorted naive conventional αβ T cells ($CD44^{lo}$ $CD25^-$ $NK1.1^-$) and obtained identical results (Fig. 3d-f). Taken together, these data demonstrate a link between CD5 expression, intrinsic strength of IL-2 and pERK responses and basal signaling in polyclonal T cells, validating the observation made in LLO56 and LLO118 T cells.

Confirmation that CD5 expression reflects self-reactivity

We sought to ascertain the association made between CD5 expression and the self-reactivity of the LLO56 and LLO118 TCRs with an independent assay. Ectopic expression of the human voltage-gated sodium channel (VGSC) genes SCN4B and SCN5A was shown to give AND transgenic T cells the ability to respond to gp250/I-E^k, its endogenous selecting pMHC ligand[22]. We reasoned that this gain-of-function approach could be extended to gauge the self-reactivity of T cells with unknown selecting ligands. To do this, we cultured VGSC-transfected LLO56, LLO118 and B6 $CD4^+$ T cells with or without irradiated B6 APCs, and analyzed their activation by upregulation of CD69. $VGSC^+$ cells were identified as those cells transfected with SCN4B-mCherry and SCN5A-GFP constructs, and thus coexpress the fluorescent markers from both constructs. Further gating on the transgenic TCR and the congenic markers allowed unequivocal identification of the different $VGSC^+$ T cell populations (Supplementary Fig. 4a).

Upon culture with B6 APCs, $VGSC^+$ LLO56 T cells showed greater CD69 upregulation than $VGSC^+$ LLO118 T cells, as would be predicted based on their respective CD5 expression (Supplementary Fig. 4b). $VGSC^+$ B6 $CD4^+$ T cells, whose mean CD5 expression lies between LLO56 and LLO118 (Supplementary Fig. 1b) showed intermediate CD69 upregulation. $VGSC^+$ B6, LLO56, and LLO118 T cells showed equivalent CD69 upregulation responses to B6 APCs pretreated with anti I-A^b. The anti-I-A^b-blocking did not reduce the response to APC to the baseline seen in the no APC controls, suggesting either incomplete blockade of MHC class II or unanticipated reactivity to other self-molecules that

was similar for all groups. CD69 upregulation was not observed in untransfected cells or SCN4B-mCherry single transfectants when cultured with B6 APCs. Further, the extent of CD69 upregulation among $VGSC^+$ T cells cultured with B6 APCs was not correlated with the expression of the channel subunits (Supplementary Fig. 4c). These results provide additional support to our conclusion that the $CD5^{hi}$ LLO56 T cells react more strongly to self-pMHC than LLO118.

Stronger intrinsic LLO56 responses emerge upon positive selection

Because T cell development is predicated on TCR interactions with self-pMHC, we reasoned that analysis of thymic selection would yield important insights into the origin of the LLO56 and LLO118 T cells biology. LLO56 thymi had markedly higher frequencies and numbers of CD4SP thymocytes than LLO118 thymi (Fig. 4a), but fewer total thymocytes. Together with the considerably larger population of $TCR^{hi}CD69^+$ post-selection thymocytes (Supplementary Fig. 5a), this observation suggested that LLO56 DP thymocytes were more efficiently positively selected than LLO118. Consistently, post-selection LLO56 thymocytes had higher expression of CD5 and CD69, two markers upregulated in response to the strength of the selecting signal (Fig. 4b). That LLO118 received a weaker signal from self-pMHC than LLO56 suggests that the lower frequency of LLO118 CD4SP thymocytes was not due to negative selection.

To explore if positively selecting TCR interactions with self-pMHC ligands in the thymus determine the intrinsic IL-2 responses of the LLO56 and LLO118 T cells, we stimulated LLO56 and LLO118 thymocytes with P+I and analyzed their IL-2 production at each developmental stage. We detected similarly high frequencies of IL-2-producing cells among LLO56 and LLO118 DN thymocytes (Fig. 4c). Any contribution of NK, NKT and γδ T cells to this IL-2 response was negligible given their low frequencies (Supplementary Fig. 5b). LLO56 and LLO118 DP thymocytes were similarly refractory to stimulation by P+I (Fig. 4c). However, as DP thymocytes transitioned to the CD4SP stage, we observed that a higher frequency of LLO56 CD4SP thymocytes produced IL-2, had higher ERK phosphorylation and basal p21 TCRζ phosphorylation compared to LLO118 CD4SP thymocytes, reproducing the difference seen in mature LLO56 and LLO118 T cells (Fig. 4c-e and Supplementary Fig. 5c).

To further test the concept that the selecting MHC environment impacts the intrinsic IL-2 responses of mature $CD4^+$ T cells, we took advantage of the fact that AND TCR transgenic T cells are selected strongly in $H\text{-}2^k$ mice and more weakly in $H\text{-}2^b$ mice[23]. This allowed us to investigate whether different intrinsic functionality could be observed from T cells expressing the same TCR, but which had developed on different MHC backgrounds. Indeed, AND T cells selected on $H\text{-}2^k$ MHC had markedly stronger intrinsic IL-2 responses than cells selected on $H\text{-}2^b$ MHC (Supplementary Fig. 5d). Taken together with the data from the LLO56 and LLO118 mice, our results demonstrate that intrinsic T cell responsiveness is set during T cell development in proportion to the strength of the selecting signals from self-pMHC.

Finally, we considered that if stronger TCR signaling in LLO56 T cells predisposed them to TCR-driven cell death *in vivo*, a greater propensity to undergo cell death might be evident in

post-selection LLO56 cells, having emerged alongside its greater basal TCR signaling. We tested this idea by stimulating LLO56 and LLO118 thymocytes and peripheral T cells with αCD3+αCD28 in culture. While pre-selection LLO118 cells showed greater cell death than LLO56, this pattern reversed in post-selection and peripheral T cells (Fig. 4f). The cell death responses seen in pre- and post-selection LLO56 and LLO118 cells were associated with basal TCRζ phosphorylation (Fig. 4e), with higher average per cell p21-TCRζ expression seen when greater cell death was observed. Developmentally acquired differences in IL-7Rα and Bcl-2 expression could not explain this abrupt shift in cell death behavior (Supplementary Fig. 5e). While the expression level of Bim was higher in LLO56 CD4SP thymocytes, this difference did not persist in peripheral cells, making it an unlikely contributor to the greater cell death observed in that setting. Thus, the increased propensity of LLO56 compared to LLO118 T cells to undergo cell death paralleled the emergence of increased basal TCR signaling in LLO56 T cells. That cells experiencing stronger TCR signals were more susceptible to cell death is in agreement with previous work[19].

Peripheral self-pMHC maintains intrinsic LLO T cell responsiveness

After leaving the thymus, T cells continue to receive tonic self-pMHC signals in the periphery. We next assessed whether deprivation of self-pMHC compromised $CD4^+$ T cell responses beyond the most proximal TCR signaling components. To do this, we analyzed LLO56 and LLO118 T cell IL-2 responses to P+I *ex vivo* after adoptively transferring the cells to B6 or MHC class II-deficient recipients for 4 days. Cells transferred to MHC class II-deficient mice had similar expression of CD3, CD4 or TCR as cells transferred to B6 mice, but they did have reduced expression of CD5 (Supplementary Fig. 6a), as might be expected for a molecule dynamically regulated by TCR-self-pMHC signals[24, 25].

Following transfer to B6 mice, LLO56 T cells showed stronger IL-2 responses to P+I than LLO118 T cells, as observed with freshly isolated cells. However, transfer to MHC class II-deficient mice rendered both LLO56 and LLO118 T cells poorly responsive to P+I (Fig. 5a). To exclude the possibility that the absence of $CD4^+$ T cells in MHC Class II-deficient recipients contributed to the reduced IL-2 responses, we analyzed the IL-2 responses of LLO56 and LLO118 T cells that were transferred to two additional sets of recipients: TCR Cα-deficient mice, which have normal MHC class II but lack αβ T cells, and H-2M-deficient mice, which have αβ T cells but whose repertoire of MHC class II bound self-peptides is largely restricted to the invariant-chain derived CLIP peptide. The goal of these additional transfer experiments was to dissect whether self-pMHC ligands or bystander αβ T cells regulate the intrinsic IL-2 responses of LLO56 and LLO118 T cells.

Following 4-day transfer to TCR Cα-deficient recipients, LLO56 T cells showed greater IL-2 production than LLO118 in response to P+I, as observed in freshly isolated cells and in cells transferred to B6 mice. However, transfer to H-2M-deficient mice rendered both LLO56 and LLO118 cells poorly responsive to stimulation, as observed with transfers to MHC class II-deficient mice (Supplementary Fig. 6b). These results indicate that the intrinsic strength of LLO56 and LLO118 T cell IL-2 responses are actively maintained by TCR-self-pMHC interactions.

We next assessed the kinetics of the loss of intrinsic IL-2 responses upon self-pMHC withdrawal. We focused on LLO56 T cells for these experiments, as the large dynamic range of IL-2 responses between LLO56 T cells deprived and not deprived of class II MHC was most appropriate to resolve changes in IL-2 responses over time. We transferred LLO56 T cells into H-2M-deficient mice for 1, 2 and 4 days, then purified and activated the cells with P+I. Compared to freshly isolated LLO56 T cells, LLO56 T cells deprived of self-pMHC for 1 day showed a sharp decline in IL-2 response to P+I, with a more subtle decline thereafter (Supplementary Fig. 6c). Thus, intrinsic IL-2 responses decay rapidly in the absence of self-pMHC ligands.

We next asked whether deprivation of self-pMHC ligands affected ERK activation. LLO56 T cells transferred to MHC class II-deficient recipients showed reduction in ERK phosphorylation compared to LLO56 T cells transferred to B6 mice (Fig. 5b). The same was true when we compared ERK phosphorylation in LLO118 T cells transferred to MHC class II-deficient and B6 mice, though the reduction in ERK phosphorylation upon MHC class II withdrawal was more modest for LLO118 T cells than seen with LLO56 T cells (Fig. 5b). These experiments provide evidence that the signal from self-pMHC impacts TCR signaling as far downstream as ERK.

Finally, we tested whether deprivation of self-pMHC signals affects the LLO56 and LLO118 T cell responses to *Listeria in vivo*. To do this, we transferred LLO56 and LLO118 T cells to B6 or MHC class II-deficient mice, generating pools of cells that were either deprived or not deprived of MHC Class II. These cells were then transferred into cohorts of B6 mice that had been infected with *Listeria* the previous day. Adoptive transfers were timed so that T cells were introduced to the infected mice at 1.5 days post-infection, at which point *Listeria* antigen presentation is abundant in the spleen[26]. The intravenously transferred LLO T cells would home to the spleen first, promoting rapid encounter of LLO-A^b complexes. Overall expansion of the transferred cells was then assessed at day 7 post-transfer (Supplementary Fig. 6d). The goal of this system was to encourage the transferred cells to activate before they have the chance to regain tonic signal from the self-pMHC normally present in B6 mice.

LLO56 T cells deprived of MHC class II expanded considerably less than

LLO56 T cells that were not deprived of MHC class II at day 7 post-T cell transfer to *Listeria*-infected B6 mice (Fig. 5c). The responses of LLO118 T cells at day 7 post-transfer were similarly strong whether the cells were deprived of self-pMHC or not (Fig. 5c). These data demonstrate that deprivation of TCR-self-pMHC interactions can impact $CD4^+$ T cell responses to pathogen *in vivo*; the common theme in this and our other self-pMHC withdrawal experiments was that LLO56 T cells, which receive stronger tonic signaling from self-pMHC than LLO118 cells, showed greater functional deficits when deprived of these signals.

CD5 feedback inhibition of LLO T cell self-reactivity

It remains unclear whether CD5 itself influences the intrinsic strength of IL-2 responses or is merely a marker for TCR-self-pMHC avidity. The literature provides conflicting data

regarding whether CD5 augments or interferes with TCR signaling, and in what contexts[16,27-29]. To address this issue, we generated LLO56 and LLO118 mice deficient in CD5. CD5-deficient LLO56 thymocytes perceived a stronger signal from self-pMHC than wild-type LLO56, as judged by their higher CD69 expression at the CD4SP stage (Fig. 6a). The greater self-reactivity of CD5-deficient LLO56 T cells may be mitigated by compensatory reductions in the expression of the TCR and CD3 in post-selection cells. Conversely, CD5-deficient LLO118 thymocytes did not show higher post-selection CD69 expression compared to wild-type LLO118 thymocytes, and peripheral CD5-deficient LLO118 T cells did not show reduced surface expression of TCR or CD3 (Fig. 6b).

Upon stimulation, CD5-deficient LLO56 and LLO118 T cells had markedly higher IL-2 responses than their wild-type counterparts (Fig. 6c), which was associated with moderate increases in ERK signaling (Fig. 6d). These findings support the view that CD5 antagonizes self-pMHC signals from the TCR, reducing the intrinsic IL-2 responsiveness maintained by TCR-self-pMHC interactions, effectively ruling out the possibility that the reduction in CD5 expression seen in the MHC class II deprivation experiments caused the observed reductions in IL-2 and pERK responses. That the cells with the strongest IL-2 responses had the highest CD5 expression suggests that this molecule does not impose a dominant inhibitory tone. Rather, since the expression of CD5 is set and maintained based on the strength of TCR-self-pMHC interactions, CD5 is positioned to impose feedback inhibition on TCR signaling to restrain the most strongly self-reactive cells[30].

Discussion

There has been great interest in understanding the factors that determine the fate and function of developing T cells in the thymus. For conventional αβ T cells, iNKT cells and T_{reg} cells[31-33], considerable evidence has demonstrated that TCR interaction with self-ligands provides essential instructive signals that drive maturation into these lineages. It is fascinating that what the TCR “sees” can guide an uncommitted thymocyte toward one of a variety of cell types with disparate effector functions. This begs the question of how TCR recognition of self-ligands induces distinct developmental signals leading to such profoundly different fates.

In this study, we demonstrated unanticipated intrinsic differences in the IL-2 responses of the pathogen-responsive LLO56 and LLO118 T cells, which originate and are actively maintained by TCR avidity for self-pMHC. The basis for how TCR recognition of self-pMHC molecules gives rise to differential intrinsic responsiveness remains elusive. In the absence of known selecting ligands, it is difficult to speculate about whether binding strength or ligand availability affects LLO56 and LLO118 TCR self-reactivity, or whether the TCRs recognize the same or different self-ligands. Assuming TCRs bind self- and cognate-pMHC with a similar docking orientation, it is plausible that the highly dissimilar CDR3β regions of LLO56 and LLO118 could mediate differential interaction with self-peptides.

Signals derived from TCR ligation of self-pMHC complexes has generally been studied using surrogate markers like CD5, or by analyzing basal activation of proximal TCR

signaling pathway components like TCRζ[17, 20, 21]. The impact of self-pMHC on signaling further downstream of the TCR has received less attention, but might be expected given the many aforementioned functions of TCR-self-pMHC interactions[4-8]. Recently, it was shown that B cells receiving a stronger signal from endogenous antigen gave stronger calcium responses upon stimulation, but similar behavior was not observed in T cells, mirroring the results of our own calcium flux experiments[34]. Using PMA to provoke responses far downstream of the TCR, we directly linked the strength of pERK responses with TCR-self-pMHC avidity. Thus, TCR ligation of self-pMHC complexes impacts the signaling of mature T cells to such an extent that even PMA stimulation cannot bypass its influence. An interesting mechanistic possibility for this draws from the demonstration that strong selecting signals from self-pMHC could promote localizion of ERK to the plasma membrane[35]. Applying this concept to our system, stronger signals from self-pMHC in peripheral LLO56 T cells could better facilitate assembly of signaling components to the plasma membrane[21], thus coordinating and strengthening ERK activation.

Our study provides evidence that withdrawal of self-pMHC can impact a $CD4^+$ T cell response to infection *in vivo*. However, one might expect that if propensity to cell death tracked with stronger basal signaling, self-pMHC withdrawal would mitigate the amount of cell death seen, leading to improved rather than exacerbated *in vivo* expansion of LLO56 T cells. That LLO56 T cells nevertheless expanded to a lesser extent than LLO118 cells suggested that the same cell-death driven differences in expansion were manifest in the self-pMHC withdrawal model as in the original adoptive transfer model[18]. It is possible that even if LLO56 T cells' basal signaling and proclivity to cell death were to be reset by an initial withdrawal of MHC class II, it could eventually rebound in the presence of self-pMHC in B6 mice over the duration of the experiment.

Finally, a recent report concluded that $CD4^+$ T cell self-reactivity correlates with affinity for cognate pMHC and efficacy in responding to pathogen[17]. Our studies with the LLO56 and LLO118 T cells, which differ strikingly in their self-reactivity yet have identical affinities for LLO/I-A^b, challenge the generality of correlations between self- and foreign-pMHC reactivity. It is a plausible idea that if selection favors TCRs able to recognize general structural features of pMHC complexes, the resulting repertoire would be enriched with TCRs that might more strongly bind any particular pMHC. However, the repertoire is nevertheless anticipatory with respect to the innumerable variety of foreign peptides that might be encountered. There is no direct selective pressure dictating that the handful of TCRs able to bind a specific set of pathogen-derived epitopes must have a particular avidity for self-pMHC beyond that necessary to get the cell through selection. Thus, as evidenced by LLO56 and LLO118 T cells, we would expect that T cells with sufficient affinity for foreign pMHC could be found across the spectrum of CD5 expression.

Several recent reports also suggest that greater TCR avidity for cognate- or self-pMHC is not necessarily a property of effective *in vivo* responses. A high frequency of $CD4^+$ T cells with undetectable binding to LCMV GP(61-80)/I-A^b (foreign antigen) or MOG(35-55)/I-A^b (self-antigen) pMHC tetramers were shown to have detectable, specific binding when assessed by *in situ* binding kinetic measurements[36, 37]. These low-affinity GP- and MOG-specific T cells were significant contributors of effector cytokines during primary LCMV

infection and EAE, respectively, which argues against the premise that the T cells with the highest affinity TCRs for foreign- or self-pMHC dominate immune responses. Two recent studies demonstrated that the duration of TCR-cognate pMHC interactions, rather than overall affinity, was the most predictive parameter for effector[38] and memory[39] differentiation of $CD4^+$ T cells. Finally, Ly-$6C^-$ $CD4^+$ T cells were shown to be enriched in $CD5^{hi}$ cells that preferentially developed into induced T_{reg} cells during immune responses, and exhibited poorer *in vivo* expansion than their Ly-$6C^{hi}$ $CD5^{lo}$ counterparts[40]. These and our studies demonstrate the complexity of what properties of TCR-pMHC interactions make for more effective $CD4^+$ T cells responses, complexity which is not accounted for by a model correlating TCR binding of foreign- and self-pMHC to the magnitude of the response.

Indeed, the quality of $CD4^+$ T cell responses involves the interplay of a number of contributing factors. Our work underscores the importance of TCR-self-pMHC interactions in determining the inherent responsiveness to stimulation and basal signaling in T cells, with implications for the performance of $CD4^+$ T cells *in vivo*. We conclude that thymic education is a critical inflection point about which these intrinsic functional attributes are determined.

Online Methods

Mice

The LLO56/B6.Thy1.1/*Rag1*$^{-/-}$ and LLO118/B6.Ly5.1/*Rag1*$^{-/-}$ TCR transgenic mice (referred to simply as LLO56 and LLO118, respectively) were described previously[18]. Briefly, the $CD4^+$ T cells in the LLO56 and LLO118 mice express a single, distinct Vα2-Vβ2 TCR that recognizes Listeriolysin O (LLO) residues 190-205 bound to I-A^b. The LLO56 and LLO118 mice were maintained as heterozygotes for the TCR transgenes. B6 and MHC class II-deficient mice were obtained from The Jackson Laboratory. CD5-deficient mice were obtained as part of the NIAID Exchange Program from the transgenic mouse repository maintained by Taconic. Mice doubly deficient for H-2M and β2m were provided by Jenny Ting's laboratory; these mice were backcrossed to B6, and the F1 progeny intercrossed to restore the wild-type β2m alleles, thus generating the H-2M-deficient mice used in this study. AND $RAG^{k/k}$, $AND^{b/b}$, and TCR Cα-deficient mice from our colony were also used in some of the described experiments. All mice were between 4 and 12 weeks of age at the beginning of each experiment, with all experimental comparisons done without blinding between age- and sex-matched cohorts. As they are extensively backcrossed, all age- and sex-matched mice of a given strain were treated as identical and assigned randomly to treatment groups. Breeding, housing and care of all mice was done in specific pathogen-free facilities under a protocol approved by the Washington University Animal Studies Committee.

Antibodies and other reagents

For flow cytometry, the following antibodies (clones indicated in parentheses) were purchased from either BD Biosciences, Biolegend, eBioscience, or Invitrogen: CD4 (clones RM4-4, RM4-5 and GK1.5), CD8 (53-7.8), CD5 (53-7.3), CD69 (H1.2F3), CD25 (PC61), B220 (RA3-6B2), F4/80 (BM8), CD11b (M1/70), CD11c (N418), IL-2 (JES6-5H4), PD-1

(J43), PD-L1 (MIH5), CD28 (37.51), CTLA-4 (UC10-4F10-11), Thy1.1 (HIS51), Ly5.1 (A20), CD3ε(145-2C11), Vα2 TCR (B20.1), γδ TCR (GL3), NK1.1 (PK136), CD44 (IM7), CD127 (SB/199), I-A^b (KH74) and Bcl-2 (3F11). Rabbit antibodies against phospho-ERK1/2 (clone D13.14.4E, also used for immunoblots) and Bim (clone C34C5), rabbit IgG isotype control (clone DA1E), and Alexa-647 conjugated anti-rabbit IgG F(ab')2 were obtained from Cell Signaling Technologies. Annexin V was obtained from BD Biosciences, and 7AAD was obtained from Sigma-Aldrich.

For immunoblots, the following primary antibodies were used: anti-p-Tyr (4G10, Upstate Biotechnology), anti-IκBα (Cell Signaling), anti-β-actin (Biolegend). Polyclonal rabbit anti-TCRζ serum 777, which recognizes unphosphorylated and phosphorylated TCRζ, was generated in our laboratory as described[41].

Analyses of T cell activation

For activation marker upregulation, ELISA, and cytokine capture assays, LLO56 and LLO118 $CD4^+$ T cells purified by magnetic bead negative selection were cultured with T cell-depleted B6 splenocytes at a 1:4 ratio. Stimulations were performed in duplicate or triplicate wells in DMEM + 10% FCS (HyClone) at 37°C/5% CO_2. The mouse cytokine capture assay was obtained from Miltenyi Biotec and done according to their protocol, except that culture media contained bovine rather than murine serum. For this assay, αCD3+αCD28 was used for stimulation; PMA + ionomycin was not used with this assay to avoid cytokine capture *in trans* by non-secreting cells.

Intracellular cytokine staining was done as previously described[15]. Briefly, cells were treated with 100 ng/mL phorbol 12-myristate 13-acetate (PMA, Sigma-Aldrich) plus 1 μg/mL ionomycin (Sigma-Aldrich) and incubated for 30 minutes. All cultures were then treated with 2 μg/mL Brefeldin A (Sigma-Aldrich) and incubated for an additional 4 hours. Samples were harvested and stained for surface markers and with 7AAD, fixed in 4% paraformaldehyde in PBS, and permeabilized in FACS buffer containing 0.5% saponin (Sigma-Aldrich), then stained for cytokines.

Surface Plasmon Resonance

Binding experiments were done with a Biacore 2000 SPR instrument essentially as described[42]. Briefly, CM5 sensor chips (GE Healthcare) were activated by a 20 minute pulse of a 1:1 mix of N-hydroxysuccinimide (NHS) and 1-ethyl-3-[3-dimethylaminopropyl] carbodiimide HCl (EDC). Soluble LLO(190-205)/I-A^b was amine coupled to the chip in 20 mM sodium citrate pH 4.5 to a total response of 300 RU, after which unreacted NHS groups on the chip were blocked by a 6 minute pulse of 1M ethanolamine pH 8.5. Concentration series of soluble LLO56 and LLO118 single-chain (scTCR) in HEPES buffered saline + BSA (10 mM HEPES, 3 mM EDTA, 150 mM NaCl, 0.05% Tween-20, and 1% BSA) were injected in duplicate over the prepared flow cells at a flow rate of 30 μL/min. Specific SPR responses of LLO TCR binding to LLO(190-205)/I-A^b were obtained by first subtracting the response from injections over a flow cell coupled with unexchanged soluble I-A^b, then correcting for bulk flow effects by subtracting the response from injections of plain buffer.

Sensorgrams were fitted by BiaEvaluation software to a 1:1 Langmuir binding model to derive values for the rate constants k_d and k_a, and the dissociation constant K_D ($=k_d/k_a$).

Soluble protein preparation

Soluble, single-chain LLO56 and LLO118 scTCRs, designed as Vβ-linker-Vα constructs, were engineered by error prone mutagenesis and conformational selection of stable mutants by yeast display as described[43]. The scTCR genes were cloned into pET28a via NheI-XhoI restriction sites, placing them in-frame with a 6x-His tag. Protein expression in *E. coli* was induced with 1mM IPTG, thus generating insoluble scTCR inclusion bodies that were harvested as described[44]. Inclusion bodies were then refolded under oxidative conditions and purified by Ni bead batch purification (Qiagen) followed by S200 FPLC-size exclusion chromatography. Purified protein was concentrated using Amicon centrifugal filters and quantified by A280 using extinction coefficients of 1.690 and 1.674 for LLO56 and LLO118, respectively. For preparation of LLO/I-A^b complexes, soluble I-A^b covalently tethered to 3R peptide via a thrombin-cleavable linker was provided by Eric Huseby. 3R/I-A^b complexes were thrombin-cleaved to release the peptide, which was then exchanged with LLO(190-205) peptide by incubation in sodium carbonate buffer pH 10.5 at 37°C for 48 hours.

Phospho-ERK flow cytometry

Cells were prepared in triplicate 100μL samples in serum-free IMDM and held on ice prior to activation. Upon addition of 100μL PMA at 2X concentration (200 ng/mL), each tube was briefly mixed then placed in a 37°C water bath to begin the stimulation. Afterwards, tubes were removed from the water bath and immediately fixed by adding 200μL 4% paraformaldehyde in PBS. After 20 minutes of fixation at room temperature, tubes were filled with 4mL ice-cold 100% methanol and held at 4°C overnight. The following day, cells were washed twice, incubated with rabbit anti-phospho-ERK, then stained with Alexa 647-conjugated anti-rabbit IgG along with antibodies against relevant surface markers.

Immunoblots

Cells were stimulated as indicated at 37°C, then lysed immediately in ice-cold buffer containing 1% Nonidet P-40, 10 μg/ml leupeptin and Pepstatin A each, 1 mM PMSF, and 1 mM sodium orthovanadate. Lysates were cleared of insoluble material by centrifugation at 16000 × g for 10 min at 4°C, then mixed with Laemmli buffer, boiled for 5 min and resolved on a 12% SDS-PAGE gel. Following overnight transfer to nitrocellulose membranes (10V, 4°C), blots were blocked for 1 hour with a 1:1 mix of PBS and Odyssey Blocking Buffer (LI-COR), incubated overnight at 4°C with mouse and rabbit primary antibodies, then incubated with Alexa 680-conjugated anti-rabbit IgG (Molecular Probes) and IRDye 800-conjugated anti-mouse IgG (LICOR) secondary antibodies. All antibody incubation steps were done in 1:1 PBS + Odyssey Blocking Buffer with 0.1% Tween-20. Membranes were imaged using an Odyssey infrared scanner (LI-COR), and densitometry done using ImageJ software (NIH).

Calcium flux experiments

T cells purified by magnetic sorting were stained for 30 minutes at 37°C with 2 μM Indo-1 AM (Molecular Probes) in the presence of 0.02% Pluronic-F127. Cells were washed twice, resuspended in buffered saline containing 1mM $CaCl_2$ and 1mM $MgCl_2$ and rested at room temperature for 20-30 minutes. All samples were prewarmed to 37°C for 5 minutes immediately prior to analysis. After establishing a baseline with unstimulated cells, ionomycin was added to a final concentration of 5 μg/mL.

Flow cytometry and cell sorting

FACS analysis was conducted using a BD FACSCalibur or BD LSR II cytometer. For cell sorting, single-cell suspensions of thymus or pooled spleen and lymph nodes were stained for populations of interest using antibodies against CD4, CD8 and CD5. For sorting of B6 T cells by CD5 expression, $CD4^+$ and $CD8^+$ T cells were pre-enriched by magnetic sorting. $CD44^{hi}$, $CD25^+$ and NK1.1+ were removed as part of our sorting strategy in some experiments in order to generate populations of naive conventional $CD4^+$ and $CD8^+$ T cells. Samples were routinely co-stained with 7AAD and antibodies against CD11b, CD11c, B220 and F4/80 to facilitate exclusion of dead and unwanted cells. All cell sorting was done using a FACSAria II sorter (BD Biosciences). Data analysis for all experiments was done using FlowJo version 8.8.6 (Treestar).

Expression of human voltage gated sodium channels (VGSC) in peripheral $CD4^+$ T cells

The human SCN5A-GFP construct was a gift from Katherine Murray[45]. The cDNA encoding human SCN4B was from Origene (RC223951) and was amplified by PCR and cloned into pcDNA3.1. Peripheral $CD4^+$ T cells were isolated by magnetic sorting, and electroporated with SCN5A-GFP and SCN4B-mCherry constructs (Amaxa Nucleofector kit for primary mouse T cells). Cells were then rested for 3 h, cultured overnight with irradiated B6 APCs, and analyzed by flow cytometry for CD69 upregulation. For all experiments, analysis was done on viable $VGSC^+$ $CD4^+$ T cells, which were defined as cells successfully transfected with both plasmids ($GFP^+mCherry^+$). For MHC Class II blocking studies, APCs were pre-incubated with 10 μg/mL anti $I\text{-}A^b$ (clone KH74) at least 15 minutes prior to addition of transfected T cells.

Adoptive Transfer Experiments

LLO56 and LLO118 $CD4^+$ T cells were purified by magnetic bead negative selection. $1\text{-}3\times10^6$ LLO $CD4^+$ T cells were transferred intravenously to B6, MHC Class $II^{-/-}$, $C\alpha^{-/-}$, or $H\text{-}2M^{-/-}$recipients for 1, 2 or 4, or 6 days, depending on the experiment, then harvested and magnetically enriched as described[46]. For experiments where donor cells were assayed for IL-2 production, cell enrichment was routinely done by positive selection for their unique congenic markers, with similar results if cells were enriched by negative selection. For experiments where donor cells were assayed for phospho-ERK or transferred into *Listeria*-infected mice, cells were purified exclusively by negative selection.

CFSE labeling

Purified LLO56 and LLO118 T cells were stained with carboxyfluorescein diacetatesuccinimidyl ester (Molecular Probes) at a final concentration of 5 μM, washed three times in PBS + 0.1% BSA, then counted and used immediately in adoptive transfer experiments.

Listeria infection

Frozen stocks of *Listeria monocytogenes* strain 10403S in PBS + 20% glycerol were thawed and serially diluted to 10^4 CFU/mL in PBS. 100μL of this solution was injected retro-orbitally to give an inoculum of 10^3 CFU/mouse. Injection titers were confirmed by colony counting aliquots of injection solution plated on brain-heart infusion agar.

Statistics

Statistical testing was done as indicated in each figure legend. $P < 0.05$ was designated as the criterion for significance; *P*-values for experiments are as reported in each figure. Decisions to use the indicated statistical analyses were assisted by the results of the Shapiro-Wilk normality test and the F test (to compare variances). Sample size determinations were not done to decide on the sizes of experimental groups in this study. All statistical analyses were conducted using Prism 6 for Mac OS X (Graphpad).

Supplementary Material

Refer to Web version on PubMed Central for supplementary material.

Acknowledgments

We thank E. Huseby for providing soluble I-A^b, Q.J. Li for generating the LLO56 and LLO118 TCR transgene constructs, J. Ting for providing the H-$2M^{-/-}$ $\beta2M^{-/-}$ mice, K. Murray for providing the SCN5A-GFP construct, D. Kreamalmeyer for mouse breeding and care, S. Horvath for peptide synthesis, D. Brinja and E. Lantelme for assistance with FACS sorting and D. Donermeyer, A. Shaw, E. Unanue and E. Brown for comments on the manuscript. We also acknowledge the members of the program project (AI-071195) under which this work was initiated: A. Chakraborty, M. Davis, M. Dustin, M. Kardar, E. Pamer, A. Perelson, D. Portnoy. and A. Shaw. This work was also supported by the NIH grant AI-24157.

References

1. van der Merwe PA, Davis SJ. Molecular interactions mediating T cell antigen recognition. Annu Rev Immunol. 2003; 21:659–684. [PubMed: 12615890]
2. Davis MM, et al. Ligand recognition by alpha beta T cell receptors. Annu Rev Immunol. 1998; 16:523–544. [PubMed: 9597140]
3. Morris GP, Allen PM. How the TCR balances sensitivity and specificity for the recognition of self and pathogens. Nat Immunol. 2012; 13:121–128. [PubMed: 22261968]
4. Ernst B, Lee DS, Chang JM, Sprent J, Surh CD. The peptide ligands mediating positive selection in the thymus control T cell survival and homeostatic proliferation in the periphery. Immunity. 1999; 11:173–181. [PubMed: 10485652]
5. Krogsgaard M, et al. Agonist/endogenous peptide-MHC heterodimers drive T cell activation and sensitivity. Nature. 2005; 434:238–243. [PubMed: 15724150]
6. Lo WL, et al. An endogenous peptide positively selects and augments the activation and survival of peripheral CD4+ T cells. Nat Immunol. 2009; 10:1155–1161. [PubMed: 19801984]

7. Kirberg J, Berns A, von Boehmer H. Peripheral T cell survival requires continual ligation of the T cell receptor to major histocompatibility complex-encoded molecules. J Exp Med. 1997; 186:1269–1275. [PubMed: 9334366]
8. Cho JH, Kim HO, Surh CD, Sprent J. T cell receptor-dependent regulation of lipid rafts controls naive CD8+ T cell homeostasis. Immunity. 2010; 32:214–226. [PubMed: 20137986]
9. Kersh GJ, et al. Structural and functional consequences of altering a peptide MHC anchor residue. J Immunol. 2001; 166:3345–3354. [PubMed: 11207290]
10. Hataye J, Moon JJ, Khoruts A, Reilly C, Jenkins MK. Naive and memory CD4+ T cell survival controlled by clonal abundance. Science. 2006; 312:114–116. [PubMed: 16513943]
11. Obar JJ, Khanna KM, Lefrancois L. Endogenous naive CD8+ T cell precursor frequency regulates primary and memory responses to infection. Immunity. 2008; 28:859–869. [PubMed: 18499487]
12. Malherbe L, Hausl C, Teyton L, McHeyzer-Williams MG. Clonal selection of helper T cells is determined by an affinity threshold with no further skewing of TCR binding properties. Immunity. 2004; 21:669–679. [PubMed: 15539153]
13. Busch DH, Pamer EG. T cell affinity maturation by selective expansion during infection. J Exp Med. 1999; 189:701–710. [PubMed: 9989985]
14. Moon JJ, et al. Naive CD4(+) T cell frequency varies for different epitopes and predicts repertoire diversity and response magnitude. Immunity. 2007; 27:203–213. [PubMed: 17707129]
15. Zehn D, Lee SY, Bevan MJ. Complete but curtailed T-cell response to very low-affinity antigen. Nature. 2009; 458:211–214. [PubMed: 19182777]
16. Azzam HS, et al. CD5 expression is developmentally regulated by T cell receptor (TCR) signals and TCR avidity. J Exp Med. 1998; 188:2301–2311. [PubMed: 9858516]
17. Mandl JN, Monteiro JP, Vrisekoop N, Germain RN. T cell-positive selection uses self-ligand binding strength to optimize repertoire recognition of foreign antigens. Immunity. 2013; 38:263–274. [PubMed: 23290521]
18. Weber KS, et al. Distinct CD4+ helper T cells involved in primary and secondary responses to infection. Proc Natl Acad Sci U S A. 2012; 109:9511–9516. [PubMed: 22645349]
19. Lenardo M, et al. Mature T lymphocyte apoptosis--immune regulation in a dynamic and unpredictable antigenic environment. Annu Rev Immunol. 1999; 17:221–253. [PubMed: 10358758]
20. Hochweller K, et al. Dendritic cells control T cell tonic signaling required for responsiveness to foreign antigen. Proc Natl Acad Sci U S A. 2010; 107:5931–5936. [PubMed: 20231464]
21. Stefanova I, Dorfman JR, Germain RN. Self-recognition promotes the foreign antigen sensitivity of naive T lymphocytes. Nature. 2002; 420:429–434. [PubMed: 12459785]
22. Lo WL, Donermeyer DL, Allen PM. A voltage-gated sodium channel is essential for the positive selection of CD4(+) T cells. Nat Immunol. 2012; 13:880–887. [PubMed: 22842345]
23. Kaye J, Kersh G, Engel I, Hedrick SM. Structure and specificity of the T cell antigen receptor. Semin Immunol. 1991; 3:269–281. [PubMed: 1724735]
24. Moran AE, et al. T cell receptor signal strength in Treg and iNKT cell development demonstrated by a novel fluorescent reporter mouse. J Exp Med. 2011; 208:1279–1289. [PubMed: 21606508]
25. Smith K, et al. Sensory adaptation in naive peripheral CD4 T cells. J Exp Med. 2001; 194:1253–1261. [PubMed: 11696591]
26. Skoberne M, Holtappels R, Hof H, Geginat G. Dynamic antigen presentation patterns of Listeria monocytogenes-derived CD8 T cell epitopes in vivo. J Immunol. 2001; 167:2209–2218. [PubMed: 11490007]
27. Tarakhovsky A, et al. A role for CD5 in TCR-mediated signal transduction and thymocyte selection. Science. 1995; 269:535–537. [PubMed: 7542801]
28. Zhou XY, et al. CD5 costimulation up-regulates the signaling to extracellular signal-regulated kinase activation in CD4+CD8+ thymocytes and supports their differentiation to the CD4 lineage. J Immunol. 2000; 164:1260–1268. [PubMed: 10640739]
29. Pena-Rossi C, et al. Negative regulation of CD4 lineage development and responses by CD5. J Immunol. 1999; 163:6494–6501. [PubMed: 10586041]

30. Azzam HS, et al. Fine tuning of TCR signaling by CD5. J Immunol. 2001; 166:5464–5472. [PubMed: 11313384]
31. Gapin L, Matsuda JL, Surh CD, Kronenberg M. NKT cells derive from double-positive thymocytes that are positively selected by CD1d. Nat Immunol. 2001; 2:971–978. [PubMed: 11550008]
32. Lio CW, Hsieh CS. A two-step process for thymic regulatory T cell development. Immunity. 2008; 28:100–111. [PubMed: 18199417]
33. Stritesky GL, Jameson SC, Hogquist KA. Selection of self-reactive T cells in the thymus. Annu Rev Immunol. 2012; 30:95–114. [PubMed: 22149933]
34. Zikherman J, Parameswaran R, Weiss A. Endogenous antigen tunes the responsiveness of naive B cells but not T cells. Nature. 2012; 489:160–164. [PubMed: 22902503]
35. Daniels MA, et al. Thymic selection threshold defined by compartmentalization of Ras/MAPK signalling. Nature. 2006; 444:724–729. [PubMed: 17086201]
36. Huang J, et al. The kinetics of two-dimensional TCR and pMHC interactions determine T-cell responsiveness. Nature. 2010; 464:932–936. [PubMed: 20357766]
37. Sabatino JJ Jr. Huang J, Zhu C, Evavold BD. High prevalence of low affinity peptide-MHC II tetramer-negative effectors during polyclonal CD4+ T cell responses. J Exp Med. 2011; 208:81–90. [PubMed: 21220453]
38. Tubo NJ, et al. Single naive CD4+ T cells from a diverse repertoire produce different effector cell types during infection. Cell. 2013; 153:785–796. [PubMed: 23663778]
39. Kim C, Wilson T, Fischer KF, Williams MA. Sustained Interactions between T Cell Receptors and Antigens Promote the Differentiation of CD4(+) Memory T Cells. Immunity. 2013; 39:508–520. [PubMed: 24054329]
40. Martin B, et al. Highly self-reactive naive CD4 T cells are prone to differentiate into regulatory T cells. Nat Commun. 2013; 4:2209. [PubMed: 23900386]
41. Kersh EN, Shaw AS, Allen PM. Fidelity of T cell activation through multistep T cell receptor zeta phosphorylation. Science. 1998; 281:572–575. [PubMed: 9677202]
42. Persaud SP, Donermeyer DL, Weber KS, Kranz DM, Allen PM. High-affinity T cell receptor differentiates cognate peptide-MHC and altered peptide ligands with distinct kinetics and thermodynamics. Mol Immunol. 2010; 47:1793–1801. [PubMed: 20334923]
43. Weber KS, Donermeyer DL, Allen PM, Kranz DM. Class II-restricted T cell receptor engineered in vitro for higher affinity retains peptide specificity and function. Proc Natl Acad Sci U S A. 2005; 102:19033–19038. [PubMed: 16365315]
44. Garcia KC, Radu CG, Ho J, Ober RJ, Ward ES. Kinetics and thermodynamics of T cell receptor-autoantigen interactions in murine experimental autoimmune encephalomyelitis. Proc Natl Acad Sci U S A. 2001; 98:6818–6823. [PubMed: 11391002]
45. Hallaq H, et al. Activation of protein kinase C alters the intracellular distribution and mobility of cardiac Na+ channels. Am J Physiol Heart Circ Physiol. 2012; 302:H782–789. [PubMed: 22101522]
46. Moon JJ, et al. Tracking epitope-specific T cells. Nat Protoc. 2009; 4:565–581. [PubMed: 19373228]

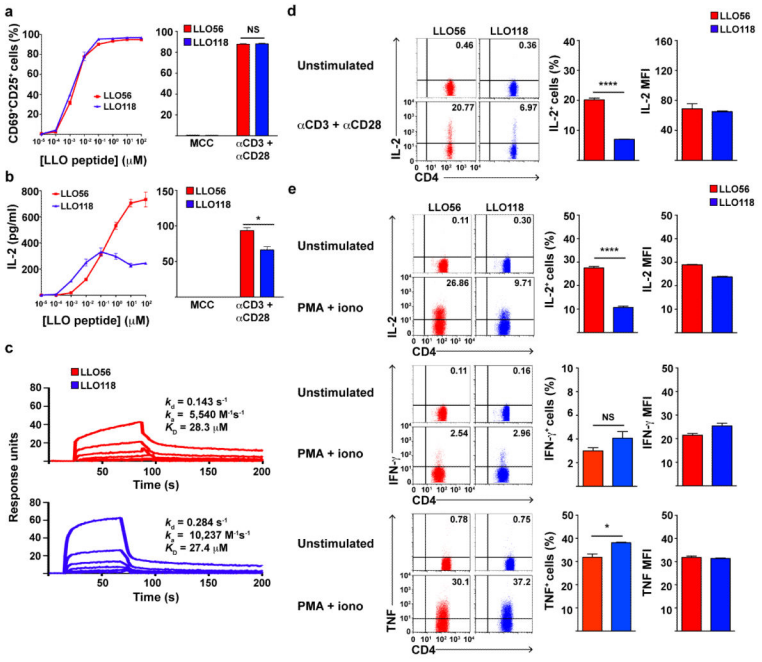

Figure 1. LLO56 and LLO118 T cells diverge in their IL-2 responses to specific or nonspecific stimuli

(a, b) Upregulation of CD69 and CD25 **(**a**)** and ELISA of IL-2 expression **(**b**)** in LLO56 and LLO118 T cells treated with indicated amounts of LLO(190-205) peptide,100 μM of MCC(83-101) peptide or 10 μg/mL αCD3 + α CD28 mAbs. **(c)** Surface plasmon resonance binding analysis of LLO56 and LLO118 scTCRs to LLO(190-205)/I-A^b. Results show a concentration series of scTCR injections beginning at 40 μM (topmost curves), with two fold serial dilutions going from top to bottom. **(d)** IL-2 capture assay of LLO56 and LLO118 CD4$^+$ T cells stimulated with 10 μg/mL αCD3 + αCD28. **(e)** Intracellular IL-2 (top), IFN-γ (middle) and TNF (bottom) assays of LLO56 and LLO118 CD4$^+$ T cells stimulated with PMA + ionomycin. For (d) and (e), primary data (left, numbers are the % cytokine$^+$ CD4$^+$ cells), graphed % cytokine$^+$ CD4$^+$ cells (middle), and graphed MFI of cytokine$^+$ CD4$^+$ cells (right) are presented. All data are representative of at least three experiments. Bar graphs depict means ± SEM, with statistical analyses done using unpaired two-tailed Student's *t* tests. **P* < 0.05, ***P* < 0.01, ****P* < 0.001, *****P* < 0.0001.

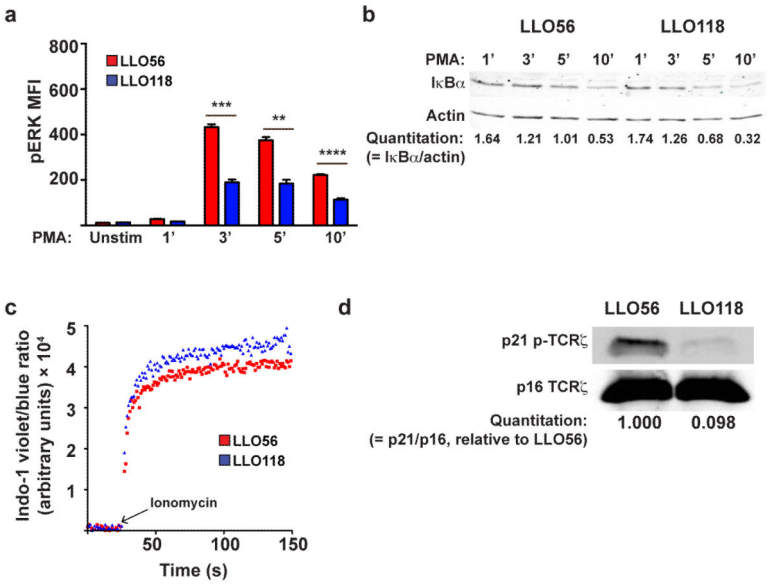

Figure 2. Stronger LLO56 IL-2 responses are linked to greater activation-induced phospho-ERK and basal phospho-TCRζ than LLO118

(a) ERK phosphorylation kinetics of PMA-stimulated LLO56 and LLO118 T cells. **(b)** IκBα degradation kinetics of PMA-stimulated LLO56 and LLO118 T cells. IκBα band densities are normalized to β-actin for quantitation. **(c)** Flow cytometric calcium flux analysis of ionomycin-treated LLO56 and LLO118 T cells, with one measurement taken every second. **(d)** Basal p21-TCRζ phosphorylation in unstimulated LLO56 and LLO118 whole cell lysates. Densities of p21 bands are normalized to p16-TCRζ, and are reported relative to LLO56. All data are representative of at least three independent experiments. Bar graphs depict means ± SEM, with statistical analysis done using unpaired two-tailed Student's *t* tests. **P* < 0.05, ***P* < 0.01, ****P* < 0.001, *****P* < 0.0001.

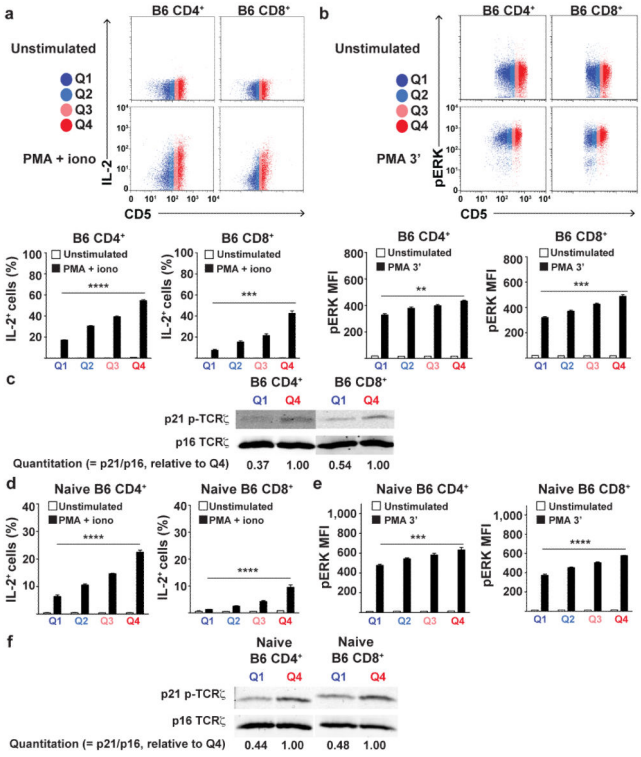

Figure 3. Strength of intrinsic IL-2 responses and signaling in polyclonal B6 CD4$^+$ and CD8$^+$ T cells correlates with CD5 expression

(a and b) CD4$^+$ and CD8$^+$ T cells were gated into four equal fractions (Q1 through Q4, from lowest to highest CD5 expression) and analyzed for IL-2 production in response to PMA + ionomycin **(**a**),** or ERK phosphorylation in response to PMA stimulation for 3 minutes **(**b**)**. Primary (upper panels) and graphed (lower panels) data are presented. **(c)** Basal TCRζ phosphorylation in whole cell lysates of unstimulated B6 CD4$^+$ and CD8$^+$ T cells FACS-sorted from the Q1 and Q4 CD5 fractions. Densities of p21 bands are normalized to p16-TCRζ, and are reported relative to Q4. (**d-f**) Analysis of IL-2 production (d), ERK phosphorylation (e) and basal TCRζ phosphorylation (f) in sorted naive conventional (CD44$^{lo\text{-}int}$, CD25$^-$, NK1.1$^-$) CD4$^+$ and CD8$^+$ T cells. All data are representative of at least three independent experiments. Bar graphs depict means ± SEM, with statistical analyses done using unpaired two-tailed Student's *t* tests. **P* < 0.05, ***P* < 0.01, ****P* < 0.001, *****P* < 0.0001.

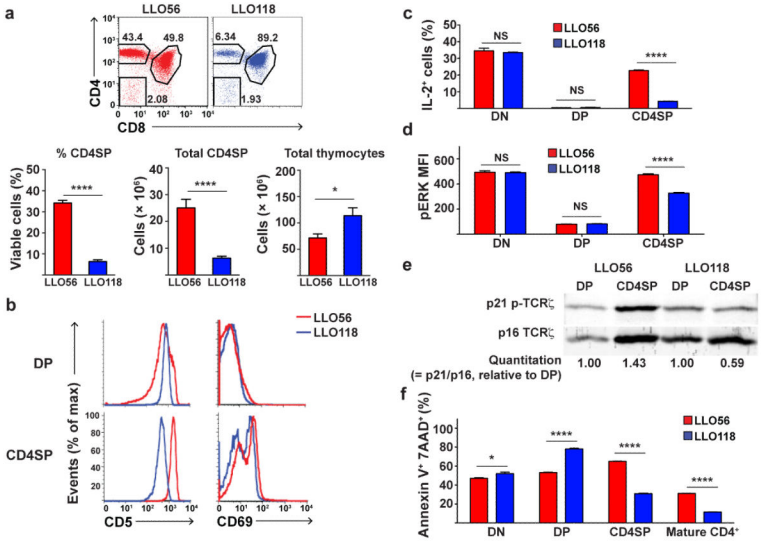

Figure 4. Functional attributes of LLO56 and LLO118 T cells emerge during positive selection, during which LLO56 receives a stronger signal from selecting self-pMHC

(a) Analysis and quantitation of LLO56 and LLO118 thymocyte subsets and total thymic cellularity, compiled from 12 (LLO118) or 13 (LLO56) thymi. **(b)** Expression of markers reflecting avidity for self-pMHC in DP (pre-selection) and CD4SP (post-selection) thymocytes, representative of at least three LLO56 and LLO118 thymi each. **(c and d)** Intracellular IL-2 analysis of PMA + ionomycin stimulated LLO56 and LLO118 thymocytes (c), and ERK phosphorylation of LLO56 and LLO118 thymocytes stimulated with PMA for 3 minutes (d), gated and analyzed by subset. Data are representative of at least three experiments. **(e)** Basal p21-TCRζ phosphorylation in FACS-sorted, unstimulated DP and CD4SP thymocytes (1.7×10^6 cells per lane) from LLO56 and LLO118 mice. Densities of LLO56 and LLO118 p21 bands are normalized to p16-TCRζ, and are reported relative to LLO56 and LLO118 DP thymocytes, respectively. Data are representative of five experiments. **(f)** Annexin V and 7AAD staining of LLO56 and LLO118 thymocyte subsets and peripheral $CD4^+$ T cells stimulated 24h with 1 μg/mL αCD3 + αCD28, representative of four experiments. Bar graphs depict means ± SEM, with statistical analyses done using unpaired two-tailed Student's *t* tests. **P* < 0.05, ***P* < 0.01, ****P* < 0.001, *****P* < 0.0001.

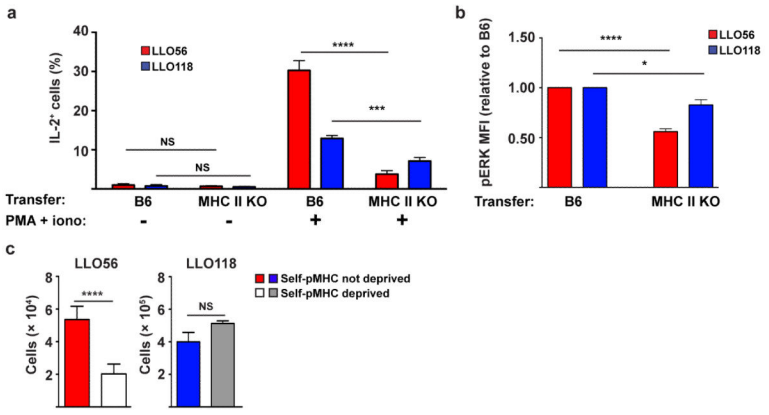

Figure 5. Deprivation of self-pMHC compromises intrinsic IL-2 and ERK responses, and *in vivo* response to *Listeria*

(a) IL-2 responses of LLO56 and LLO118 T cells transferred to B6 (LLO56 $n = 6$, LLO118 $n = 7$) or MHC II-deficient (LLO56 $n = 8$, LLO118 $n = 6$) mice for 4 days, then stimulated *ex vivo* with PMA + ionomycin. The % IL-2^+ cells from each recipient over three experiments was compiled. **(b)** Phospho-ERK responses of LLO56 and LLO118 T cells transferred to B6 (LLO56 $n = 7$, LLO118 $n = 6$) or MHC II-deficient (LLO56 and LLO118 $n = 5$) mice for 4 days, then stimulated *ex vivo* with PMA for 3 minutes. The pERK MFI of cells transferred to MHC II-deficient recipients was normalized to the pERK MFI of cells transferred to B6 recipients in the same experiment, and compiled from three or four experiments. **(c)** Expansion of LLO56 and LLO118 T cells either deprived (LLO56 $n = 12$, LLO118 $n = 6$) or not deprived (LLO56 $n = 12$, LLO118 $n = 7$) of self-pMHC at 7 days post-transfer to *Listeria*-infected B6 mice, compiled from 6 (LLO56) or 4 experiments (LLO118). Bar graphs depict means ± SEM. For (a) and (b), statistical analyses were done using unpaired two-tailed Student's *t* tests; for (d), paired two-tailed Student's *t* tests were done. $*P < 0.05$, $**P < 0.01$, $***P < 0.001$, $****P < 0.0001$.

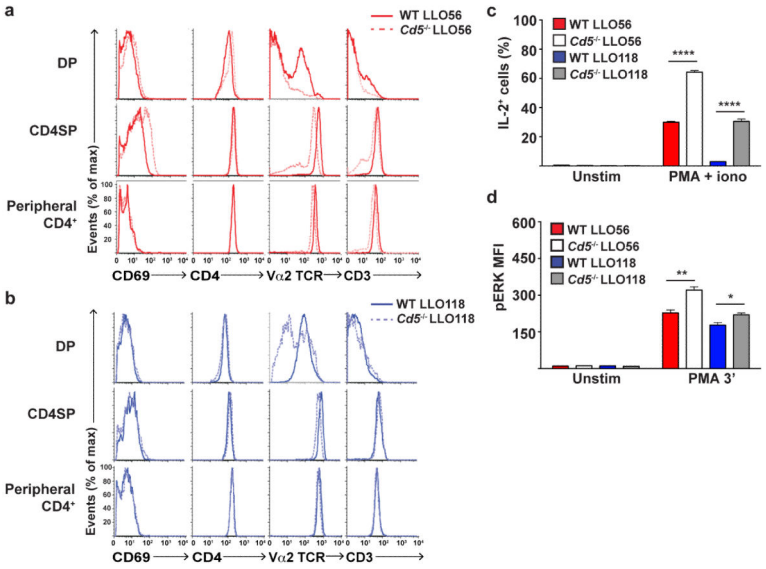

Figure 6. CD5 antagonizes signal from self-pMHC and intrinsic IL-2 and pERK responses

(a and b) Expression of functional markers in wild-type and CD5-deficient LLO56 (a) and LLO118 (b) thymocyte subsets and peripheral cells. **(c)** Intrinsic IL-2 response in wild-type and CD5-deficient LLO56 and LLO118 T cells stimulated with PMA + ionomycin. **(d)** Phospho-ERK response in wild-type and CD5-deficient LLO56 and LLO118 T cells stimulated with PMA for 3 minutes. Bar graphs depict means ± SEM, with statistical analyses done using unpaired two-tailed Student's *t* tests. Displayed data are representative of two (LLO118) or three (LLO56) experiments. **P* < 0.05, ***P* < 0.01, ****P* < 0.001, *****P* < 0.0001.

Table 1

Previously identified characteristics of LLO56 and LLO118 T cell responses to antigen *in vitro* and *in vivo*.

Measurement	**LLO56**	**LLO118**
Primary expansion to Listeria *in vivo*	+	+++
Proliferation to peptide or Listeria *in vitro*	+	+
Proliferation during primary response to Listeria *in vivo*	+	+
Cell death during primary response to Listeria *in vivo*	+++	+